Molecular Mechanism of DNA Recognition by the α Subunit of the *Oxytricha* Telomere Binding Protein†

Laurent Laporte, James M. Benevides, and George J. Thomas, Jr.*

Division of Cell Biology and Biophysics, School of Biological Sciences, University of Missouri−Kansas City, Kansas City, Missouri 64110-2499

Received August 7, 1998; Revised Manuscript Received November 16, 1998

ABSTRACT: Interactions between telomeric DNA and the α subunit of the heterodimeric telomere binding protein of *Oxytricha nova* have been probed by Raman spectroscopy, CD spectroscopy, and nondenaturing gel electrophoresis. Telomeric sequences investigated include the *Oxytricha* 3′ overhang, $d(T_4G_4)_2$, and the related sequence $dT_6(T_4G_4)_2$, which incorporates a 5′-thymidylate leader. Corresponding nontelomeric isomers, $d(TG)_8$ and $dT_6(TG)_8$, have also been investigated. Both $d(T_4G_4)_2$ and $dT_6(T_4G_4)_2$ form stable hairpins that contain Hoogsteen G·G base pairs [Laporte, L., and Thomas, G. J., Jr. (1998) *J. Mol. Biol. 281,* 261−270]. The α subunit binds specifically and stoichiometrically to the $dT_6(T_4G_4)_2$ hairpin and alters its secondary structure by inducing conformational changes in the 5′-thymidylate leader without extensive disruption of G·G base pairing. Conversely, binding of the α subunit to $d(T_4G_4)_2$ eliminates G·G pairing and unfolds the hairpin. DNA unfolding is accompanied by conformational changes affecting both the backbone and dG residues, as evidenced by Raman and CD spectra. Interestingly, the α subunit also forms complexes with the nontelomeric isomers, $d(TG)_8$ and $dT_6(TG)_8$, evidenced by altered electrophoretic mobility in nondenaturing gels; however, Raman and CD spectra of complexes of the α subunit with nontelomeric DNA suggest no significant changes in backbone or deoxynucleoside conformations. Similarly, the α subunit binds to but does not appreciably alter the secondary structure of duplex DNA. The present results show that while the α subunit has the capacity to bind to Watson−Crick and different non-Watson−Crick motifs, DNA refolding is specific to the *Oxytricha* telomeric hairpin and the retention of G·G pairing is specific to the telomeric sequence incorporating the 5′ leading sequence. A model is proposed for α subunit binding to telomeric DNA, and the physiological role of the α subunit in telomere organization is discussed.

Telomeres, the termini of eukaryotic chromosomes, are nucleoprotein assemblies designed to maintain chromosome stability, ensure accuracy in genome replication, prevent aberrant interchromosome fusion, and control cellular senescence (*1*−*4*). Recent studies have shown that telomeres of *S. cerevisiae* can selectively retard expression of proximal genes during S phase, suggesting a direct regulatory role (*5*). Additionally, evidence has been obtained that telomeres of the ciliate *Tetrahymena* can mediate the formation of interchromosome complexes during replication (*6*). Specific roles have also been proposed for telomere binding proteins in the control of telomeric DNA structure and organization in both lower eukaryotes (*7*) and humans (*8*).

The DNA component of the telomere is characterized typically by a 5′ strand that is rich in adenine and cytosine and a 3′ strand that is rich in thymine and guanine. In higher organisms, telomeric DNA comprises both a double-stranded segment ranging in size from several base pairs to tens of kilobase pairs, plus a single-stranded 3′ overhang that is capable of forming higher order secondary structures in vitro (*9*). In some organisms, the telomere is resistant to nuclease degradation, a characteristic that has been attributed to either the formation of a highly stable DNA secondary structure or the association with specific telomere binding proteins (*10*, *11*).

In the ciliated protozoan *Oxytricha nova*, the telomere binding protein is heterodimeric, comprising basic subunits of 56 kDa (α) and 41 kDa (*β*) (*12*, *13*). The α/*β* heterodimer has been shown to form ternary complexes with DNA sequences ending in the *Oxytricha* telomeric 3′ overhang dTTTTGGGGTTTTGGGG [or $d(T_4G_4)_2$][1] (*12*). The ternary complexes are stable at high ionic strength in vitro, and the bound protein is believed to protect the single-stranded 3′ overhang segment from nuclease digestion (*12*). In addition to ternary complex formation, each subunit of the *Oxytricha* telomere binding protein is capable of forming binary complexes with DNA sequences containing the $d(T_4G_4)_2$ terminus. The *β* subunit induces single-stranded telomeric DNA to fold into a parallel-stranded quadruplex structure (*14*−*16*). Biochemical assays demonstrate that the α subunit likewise binds to *Oxytricha* telomeric DNA (*17*), although structural details of an α:DNA complex have not yet been reported.

† Part LXXI in the series Raman Spectral Studies of Nucleic Acids. Supported by NIH Grant GM54378.

* To whom correspondence may be addressed.

[1] Abbreviations: Oxy2, $d(T_4G_4)_2$; T6Oxy2, $dT_6(T_4G_4)_2$; dG, deoxyguanosine; dT, thymidine or thymidylate; α subunit, 56 kDa subunit of the heterodimeric *Oxytricha nova* telomere binding protein; α:Oxy2,1:1 complex of the α subunit and Oxy2; α:T6Oxy2, 1:1 complex of the α subunit and T6Oxy2.

10.1021/bi9819024 CCC: $18.00
Published on Web 12/17/1998

To further elucidate the role of the α subunit of the *Oxytricha* telomere binding protein in telomeric DNA recognition, we have investigated complexes of α with the *Oxytricha* 3′ overhang, $d(T_4G_4)_2$ (hereafter Oxy2). Parallel studies have also been carried out on the sequence $dT_6(T_4G_4)_2$ (T6Oxy2), which incorporates a leading 5′-thymidylate segment, and on the corresponding nontelomeric isomers, $d(TG)_8$ and $dT_6(TG)_8$. In previous papers of this series, we reported Raman spectroscopic signatures, secondary structures, and thermostabilities of the α and *β* subunits (*18*), the structural basis of telomeric DNA recognition by the *β* subunit (*14*), and the solution secondary structures of Oxy2 and T6Oxy2 in the absence of telomere binding protein (*19*). In the present work, the α:DNA complexes are probed by Raman spectroscopy, CD spectroscopy, and nondenaturing gel electrophoresis. The results provide insight into conformational changes induced by α in the *Oxytricha* telomeric 3′ overhang and demonstrate a plausible role for the subunit in telomere organization. On the basis of the present findings, we propose a mechanism for α subunit binding in *Oxytricha* telomeric sequences.

MATERIALS AND METHODS

Isolation and Purification of the α Subunit. The α subunit was expressed in an *E. coli*-containing recombinant plasmid vector generously provided by Dr. Thomas R. Cech, Howard Hughes Medical Institute, University of Colorado. The α subunit was extracted from the bacteria and purified using published procedures (*18*, *20*). Typically, the preparation and purification protocol (*18*, *20*) yielded approximately 30 mg of purified α subunit. The protein was stored at −80 °C in a 50:50 vol% mixture of glycerol and 5 mM Tris buffer (pH 7.5) containing 0.5 mM EDTA and 50 mM NaCl. Prior to use, the protein was dialyzed extensively against the Tris buffer solution.

Oligonucleotide Preparation. Oligodeoxynucleotides $d(T_4G_4)_2$ (Oxy2), $dT_6(T_4G_4)_2$ (T6Oxy2), $d(TG)_8$, and $dT_6(TG)_8$ were synthesized on an Applied Biosystems Model 381A DNA synthesizer and purified as described (*21*). Purified DNA was dissolved to 15 mg/mL with milliQ water and adjusted to pH 7.2 ± 0.2 using either dilute HCl or NaOH. The final Na^+ concentration in these samples never exceeded 10 mM. Aliquots of the DNA solution were heated to 90 °C for 1.5 h, frozen immediately with liquid nitrogen, and lyophilized. Following lyophilization, each DNA was diluted to 30 mg/mL with milliQ water for spectroscopic investigation of the oligonucleotide solution conformation.

Complex Formation. Solutions of α ($\epsilon_{280} = 5.55 \times 10^4$ M^{-1} cm^{-1}) and Oxy2 (ϵ_{260}, per mole phosphate $= 1.58 \times 10^5$ M^{-1} cm^{-1}) were mixed to achieve a 1:1 molar ratio and total concentration of 50 mg/mL at pH 7.3 ± 0.1. A similar procedure was followed for mixtures of α and T6Oxy2. Sodium concentrations were maintained below 50 mM. Samples were sealed in glass capillary tubes for Raman spectroscopy.

Raman Spectroscopy. Raman spectra were excited with the 514.5 nm line of an argon ion laser (Innova-70, Coherent Inc., Santa Clara, CA) using 200 mW of radiant power at the sample. The spectra were collected on a triple spectrograph (Triplemate Model 1877, SPEX Ind., Metuchen, NJ) equipped with a liquid nitrogen-cooled charge-coupled device detector (Model LN-CCD-1152UV, Princeton Instruments, Princeton, NJ) of 1152 × 298 pixels. The effective spectral slit width was approximately 5 cm^{-1}. Samples were maintained at 9 °C for all experiments by use of a thermostat designed for the 90° scattering geometry (*22*). Further details of Raman instrumentation, sample illumination procedures, and criteria for significance of Raman difference bands have been given previously (*18*, *23*).

Circular Dichroism Spectroscopy. Circular dichroism (CD) in the region 240−360 nm was recorded on a JASCO-720 spectrophotometer with a scan speed of 20 nm/min and a response time of 1 s. Samples for CD spectroscopy were prepared in 10 mM sodium phosphate buffer at pH 7.3 ± 0.1 and thermostated at 10 °C in a cell of 0.5 cm path. Prior to spectroscopic analysis, oligonucleotides (10−15 *μ*M) were heated to 90 °C for 1.5 h and slowly cooled. The α:DNA complexes were prepared by addition of the appropriate volume of a solution of the α subunit (1.0 mM) to the oligonucleotide solution.

Nondenaturing Polyacrylamide Gel Electrophoresis. Aliquots of solutions of the α subunit and oligonucleotide, each in buffer containing 5 mM Tris (pH 7.5), 0.5 mM EDTA, and 50 mM NaCl, were combined in the appropriate stoichiometry to a total volume of ∼6 *μ*L and equilibrated at 4 °C. An aliquot (∼1 *μ*L) of dye solution (15% glycerol, 0.05% bromophenol blue) was added to each sample prior to electrophoresis. Samples were loaded onto an 8% polyacrylamide gel in 0.5 × TBE buffer (4.5 mM Tris, 4.5 mM boric acid, 0.1 mM EDTA) that had been prerun for 30 min at 110 V and 4 °C. The loaded gel was then run at 110 V and 4 °C for an additional 4 h and stained with Coomassie blue.

RESULTS AND DISCUSSION

1. Raman Signature of the α Subunit. The Raman spectrum of the α subunit of the *Oxytricha* telomere binding protein has been discussed in detail previously (*18*). The spectrum indicates a predominance of *β*-strand (40−50%) and irregular secondary structures and considerably smaller percentages of α-helix and random coil conformations.

2. Raman Signatures of Telomeric and Nontelomeric DNA. Raman spectra and H/D exchange profiles of Oxy2 and the nontelomeric isomer $d(TG)_8$ have been compared and interpreted previously (*19*, *24*). The data indicate for Oxy2 a hairpin structure containing a 5′-dT_4 leader, a stem of four G•G base pairs, and a connecting dT_4 loop, involving Hoogsteen pairing of syn dG and anti dG conformers. For $d(TG)_8$, only syn dG conformers are observed, and no hairpin is formed. The $d(TG)_8$ sequence is considered to form an extended chain at the experimental conditions employed. Analogous hairpin and extended structures, respectively, are observed for T6Oxy2 and $dT_6(TG)_8$ (*19*).

Previously reported Raman spectra of Oxy2 and T6Oxy2 (*19*) illustrate an interesting characteristic of their dG marker bands in the 600−700 and 1300−1400 cm^{-1} intervals; viz., they are consistently elevated in wavenumber value (∼6 ± 3 cm^{-1}) with respect to counterparts in $d(TG)_8$ and $dT_6(TG)_8$. Similarly elevated dG markers have been noted for quadruplex structures (*19*, *25*). A plausible explanation is that Hoogsteen N7 hydrogen bonding elevates the vibrational frequencies of these dG marker bands.

3. Raman Difference Spectra of DNA Complexes of the α Subunit. (*a*) α:*Oxy2*. In Figure 1, the Raman spectrum of

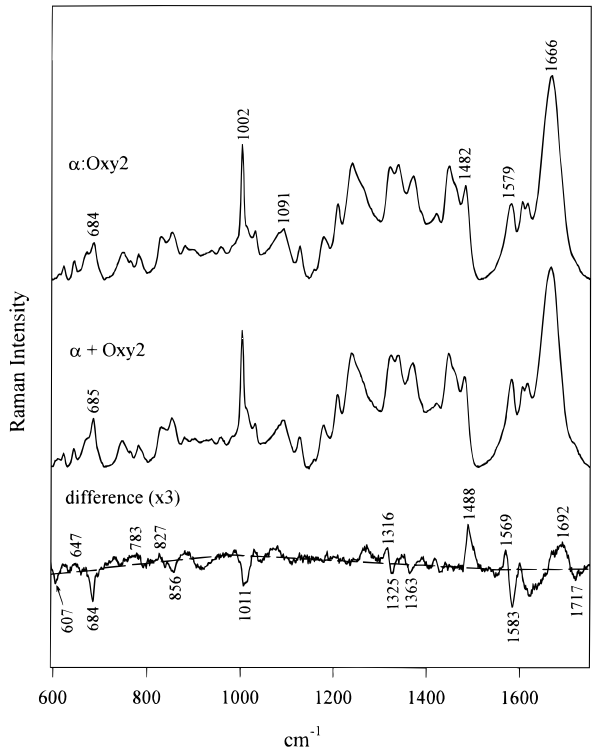

FIGURE 1: Raman spectrum in the region 600−1750 cm^{-1} of the 1:1 complex of the α subunit and Oxy2 (α:Oxy2, top), the digital sum of Raman spectra of constituents (α + Oxy2, middle), and the difference spectrum of the complex minus the sum of constituents (amplified 3-fold, bottom). Raman spectra of the separated components were published previously (*18*, *19*). Spectra were excited at 514.5 nm from solutions containing 50 mg/mL in sample buffer (5 mM Tris, pH 7.2 ± 0.1, 0.5 mM EDTA, 50 mM NaCl) at 10 °C and were corrected for small contributions from the buffer. Labels indicate wavenumber (cm^{-1}) values. Residue assignments of prominent bands discussed in the text are reported elsewhere (*18*, *19*).

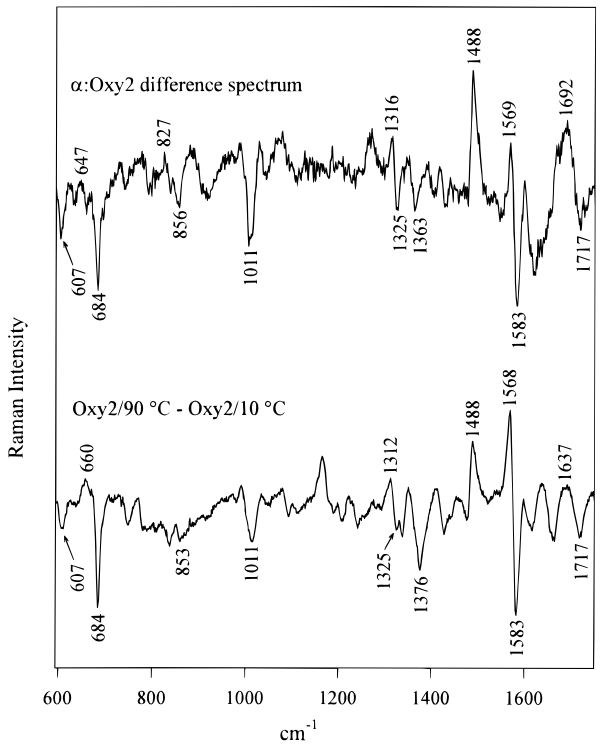

FIGURE 2: The upper trace shows the Raman difference spectrum between the 1:1 complex of the α subunit and Oxy2 and their spectral sum of constituents. The lower trace shows the Raman difference spectrum between Oxy2 at 90 and 10 °C. Other conditions are given in Figure 1.

the 1:1 complex of the α subunit and Oxy2 (α:Oxy2, top trace) is compared with the spectral sum of constituents (α + Oxy2, middle trace). The difference spectrum of the complex minus the spectral sum (Figure 1, bottom trace) exhibits many peaks and troughs, indicating that the structure of the complex differs substantially from the structures of the constituents. [Spectra of the separate components were published previously (*18*, *19*).] Interestingly, nearly all of the difference peaks and troughs of Figure 1 are assignable to Oxy2, indicating a significant structural change in DNA induced by the α subunit. The structure of the α subunit is not greatly altered by interaction with DNA, as evidenced by the absence of protein Raman markers in the Figure 1 difference spectrum and by the absence of tryptophan band shifts in fluorescence spectra (data not shown).

Comparison of the α:Oxy2 difference spectrum of Figure 1 with the previously reported difference spectrum for the complex of Oxy2 with the *β* subunit (*14*) reveals few similarities, indicating that the two subunits perturb the same telomeric DNA differently. A similar conclusion has been reached from comparative analyses of DNA footprinting and electrophoretic mobility assays of DNA complexes of the α and *β* subunits (*15*, *16*, *20*).

We have also compared the α:Oxy2 difference spectrum of Figure 1 with difference spectra obtained for thermal denaturation of the Oxy2 hairpin (*19*) (Figure 2) and for structure transformations of GT-rich B DNA and quadruplex DNA (Oxy4) (*24*). A similarity exists only with thermal denaturation of Oxy2, which is illustrated in Figure 2.

The similarity of the two difference spectra of Figure 2 encompasses many of the Raman markers of dG and dT and suggests that the effect of α subunit binding on Oxy2 structure is to unfold the hairpin, not unlike the effect of thermal denaturation. We propose that the α subunit disrupts Hoogsteen G·G pairs of Oxy2 and changes the conformation of the oligonucleotide backbone. Particular Raman features that support this interpretation are the following: (i) The intensity increase at 1488 cm^{-1} and the band shift from 1583 to 1569 cm^{-1} indicate conversion of guanine N7 hydrogen bond acceptors from Hoogsteen pairing to unpairing (*19*, *26*). (ii) The difference trough at 607 cm^{-1} is consistent with a structural change involving the dT_4 loop of Oxy2 (*19*, *21*). (iii) The trough at 1363 cm^{-1} implies a net change in guanine ring environments (*27*). (iv) The trough at 856 cm^{-1} in the α:Oxy2 difference spectrum (Figure 2, top) is similar to that of thermally unfolded Oxy2 (Figure 2, bottom). It is therefore reasonable to attribute these features to a conformational change in the Oxy2 backbone accompanying hairpin unfolding. (v) Finally, although the 1717 → 1692 cm^{-1} band shift cannot be assigned unambiguously to DNA (the protein contribution to this spectral region could be as large as the expected DNA contribution from dG and dT), it is consistent with a change in hydrogen bonding environment of guanine carbonyl acceptors (C6═O). Such a band shift is expected for a net change in environment of guanine C6═O groups from G·G pairing to solvent exposure (*19*, *24*).

Both difference spectra of Figure 2 reveal a deep trough near 1011 cm^{-1}, i.e., higher intensity of the 1011 cm^{-1} band

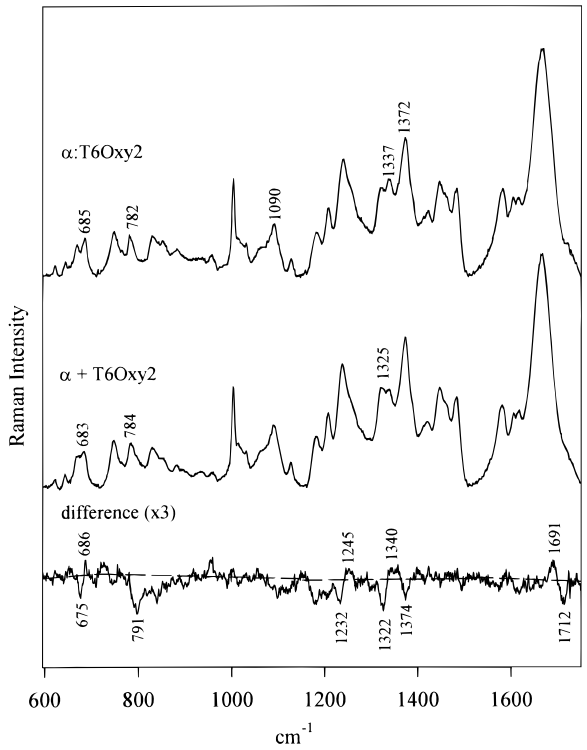

FIGURE 3: Raman spectra of the 1:1 complex of the α subunit and T6Oxy2 (α:T6Oxy2, top), the digital sum of constituents (α + T6Oxy2, middle), and their difference spectrum (amplified 3-fold, bottom). Other conditions are given in Figure 1.

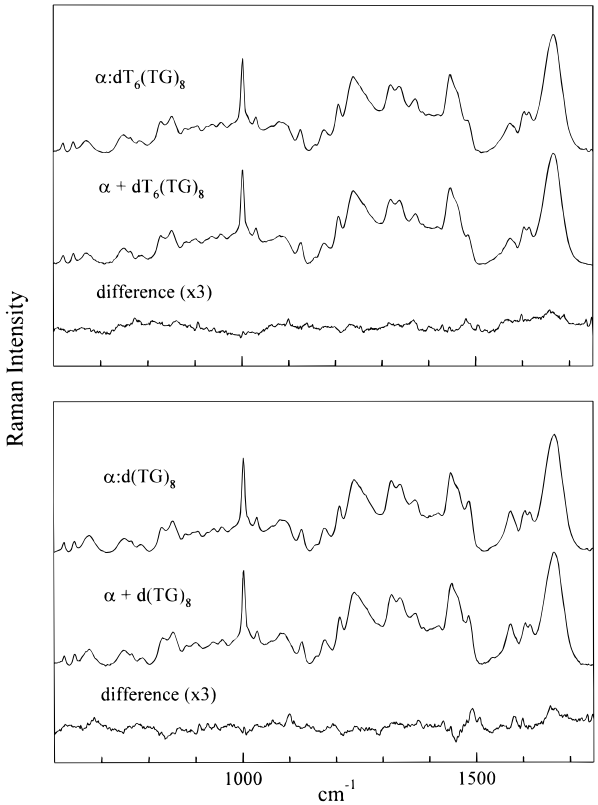

FIGURE 4: (Lower panel) Raman spectra of the 1:1 complex of the α subunit and $d(TG)_8$ [α:$d(TG)_8$, top], the digital sum of constituents [α + $d(TG)_8$, middle], and their difference spectrum (amplified 3-fold, bottom). (Upper panel) Raman spectra of the 1:1 complex of the α subunit and $dT_6(TG)_8$ [α:$dT_6(TG)_8$, top], the digital sum of constituents [α + $dT_6(TG)_8$, middle], and their difference spectrum (amplified 3-fold, bottom).

in the Oxy2 hairpin than in unfolded structures. A similar intensity difference has been observed for a structure transformation of Oxy4 (*24*). Interestingly, the enhanced intensity of the 1011 cm^{-1} band appears to be specific to telomeric DNA, as no comparable intensity change accompanies disruption of Watson−Crick G·C pairing (L. Laporte and G. J. Thomas, Jr., unpublished results).

Not all features of the two difference spectra compared in Figure 2 are equivalent, indicating that thermal and α-induced unfolding of Oxy2, though similar, are not identical. For example, the difference spectrum of thermally unfolded Oxy2 exhibits an intense trough at the position of the thymine $C5H_3$ marker near 1376 cm^{-1} (*23*, *28*), while the corresponding trough for α-unfolded Oxy2 is weaker and located at significantly lower wavenumber (1363 cm^{-1}). This suggests different environments for thymine $C5H_3$ groups in the two cases, which could be explained by more restricted solvent access to thymine methyl substituents in the α:Oxy2 complex (*19*, *23*, *28*), presumably a consequence of protein binding.

Finally, we observe that the difference spectrum representing α-induced unfolding of Oxy2 (Figure 2, top) exhibits a conspicuous trough at 1325 cm^{-1} and companion peak at 1316 cm^{-1}. A deep trough is also observed at 684 cm^{-1} with a possible companion peak near ∼650 cm^{-1}. These features are consistent with a change in dG conformation, possibly from C2′-endo/anti to C3′-endo/anti. Interestingly, the data imply little change in the overall syn/anti ratio of dG.

In summary, the α:Oxy2 difference spectrum is consistent with α-induced disruption of G·G base pairs, unfolding of hairpin secondary structure, and attendant changes in dG and dT conformations. This Oxy2 structure change is similar in many respects to that resulting from thermal denaturation.

(*b*) α:*T6Oxy2*. The Raman spectrum of the 1:1 complex of the α subunit and T6Oxy2 (α:T6Oxy2) is compared with the spectral sum of constituents (α + T6Oxy2) in Figure 3. [The Raman spectrum of the single-component T6Oxy2 and a detailed discussion of spectral band assignments are given elsewhere (*19*). The data indicate a hairpin conformation similar to that of Oxy2.] As in the case of the α:Oxy2 complex described above (Figures 1 and 2), the difference spectrum of Figure 3 reveals a perturbation of T6Oxy2 structure by α subunit binding. However, the perturbed structure of T6Oxy2 differs qualitatively from that of Oxy2. Thus, in the case of T6Oxy2, α subunit binding leads to unique Raman band shifts (675 → 686 cm^{-1} and 1322 → ∼1340 cm^{-1}) that are consistent with conversion of a small percentage (∼10−20%) of dG syn conformers to the anti conformation (*14*, *24*).

Other features of the Figure 3 difference spectrum that are unique to the α:T6Oxy2 complex (cf. Figures 1 and 3) may be interpreted as follows: (i) The intensity change at 791 cm^{-1} is consistent with a change in backbone phosphodiester conformation. A similar difference feature is observed for conformational transitions in other dT-containing polynucleotides (*14*, *29*). Because the dT residues also contribute a thymine ring mode near 790 cm^{-1}, the negative difference band may also reflect a change in thymine ring environment with α subunit binding. (ii) Interestingly, no trough occurs at 1011 cm^{-1} in Figure 3, suggesting that the T6Oxy2 telomeric hairpin is either not unfolded by α subunit

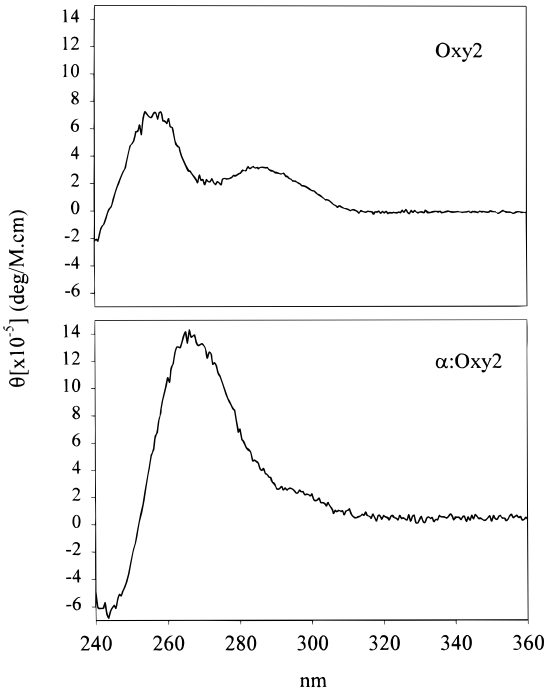

FIGURE 5: Circular dichroism spectra in the region 240−360 nm of Oxy2 (top) and the α:Oxy2 complex (bottom). Spectra were collected at 10 °C from solutions containing DNA at 11 μM in 10 mM sodium phosphate buffer at pH 7.3 ± 0.1.

binding or unfolded quite differently than in the case of Oxy2. (iii) Relatively intense difference peaks and troughs, probably associated with dT residues (*27*), occur throughout the interval 1200−1400 cm^{-1}. (iv) No prominent difference peaks or troughs occur in Figure 3 between 1400 and 1600 cm^{-1}. This is in striking contrast to Figure 1, and again is consistent with either retention of Hoogsteen G·G pairs of T6Oxy2 or replacement by comparable N7 hydrogen bonding with protein donor groups.

In summary, α subunit binding alters the secondary structure of T6Oxy2, and results in a Raman signature for the α:T6Oxy2 complex (Figure 3, bottom) differing from that of α:Oxy2 (Figure 1, bottom). In the α:T6Oxy2 complex, we find spectroscopic evidence that Hoogsteen G·G pairing is not completely disrupted. This conclusion is supported not only by the absence of difference bands at 1011, 1470−1490, and 1570−1590 cm^{-1}, but also by the fact that dG conformation markers largely retain the elevated wavenumber values associated with Hoogsteen structures (*19*, *25*) (see section *2*).

(*c*) α:*d(TG)$_8$ and* α:*dT$_6$(TG)$_8$*. The upper and lower panels of Figure 4 compare Raman spectra of the "complexes" α:dT$_6$(TG)$_8$ and α:d(TG)$_8$, respectively, with their constituents. In each case, the Raman difference spectrum indicates minimal structural perturbations. The only significant difference feature occurs near 1450 cm^{-1} for α:d(TG)$_8$ (Figure 4, bottom) and is most likely due to altered side-chain packing of the α subunit. In contrast to Oxy2 and T6Oxy2 (Figures 1 and 3), the data of Figure 4 show that α subunit binding does not appreciably alter structures of d(TG)$_8$ and dT$_6$(TG)$_8$. Both sequences are considered to form an extended chain at the experimental conditions employed, consistent with previous results (*19*).

4. Circular Dichroism Spectroscopy. Figure 5 shows CD spectra of Oxy2 (upper panel) and the α:Oxy2 complex

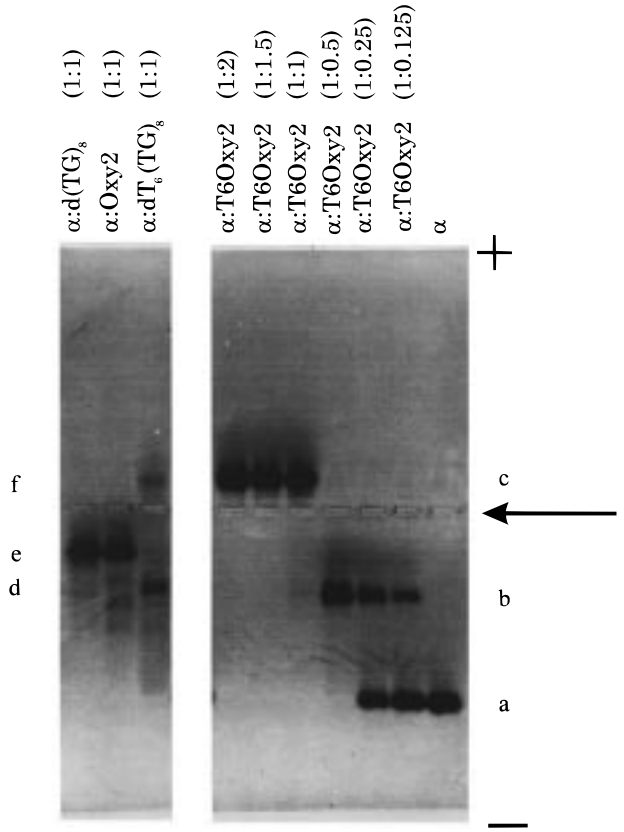

FIGURE 6: Nondenaturing protein gel mobility assay. The α subunit of the *Oxytricha* telomere binding protein was incubated with or without different telomeric and nontelomeric strands at the stoichiometric ratios shown in parentheses above the lane markers. The samples were loaded in the center of the nondenaturing gel as indicated by the arrow. Symbols + and − indicate the location of positive and negative electrodes, respectively. Band a corresponds to unbound α subunit, bands b and c to α:T6Oxy2 complexes in excess protein or DNA, respectively, bands d and f to dominant species in α:dT$_6$(TG)$_8$ complexes, and band e to α:Oxy2 and α:d(TG)$_8$ complexes.

(lower panel) in the region 240−360 nm. The CD profile of Oxy2 is similar to that reported previously (*30*, *31*), exhibiting a trough centered at 238 nm and peaks centered at 257 and 285 nm. Nondenaturing gel electrophoresis of Oxy2 (data not shown) indicates a single species of high mobility, consistent with a monomolecular foldback structure (*19*). Upon formation of the α:Oxy2 complex, the CD profile exhibits a large change, resulting in a trough at 240 nm and single peak at 266 nm. This dramatic CD change confirms that binding of the α subunit induces a substantial change in Oxy2 conformation. Similar results are obtained for the α:T6Oxy2 complex (data not shown). Conversely, CD profiles of α:d(TG)$_8$ and α:T$_6$(TG)$_8$ do not differ substantially from those of the respective protein-free oligonucleotides (data not shown).

5. Nondenaturing Gel Electrophoresis. Figure 6 shows a nondenaturing Coomassie-stained gel assay of the α subunit and of representative complexes of α with T6Oxy2, Oxy2, dT$_6$(TG)$_8$, and d(TG)$_8$. The results, while complicated, demonstrate that each DNA species is capable of forming a complex with electrophoretic mobility differing from that of the isolated α subunit. Band a characterizes the electrophoretic mobility of the free α subunit. Bands b and c represent complexes of the type α:T6Oxy2, in which the

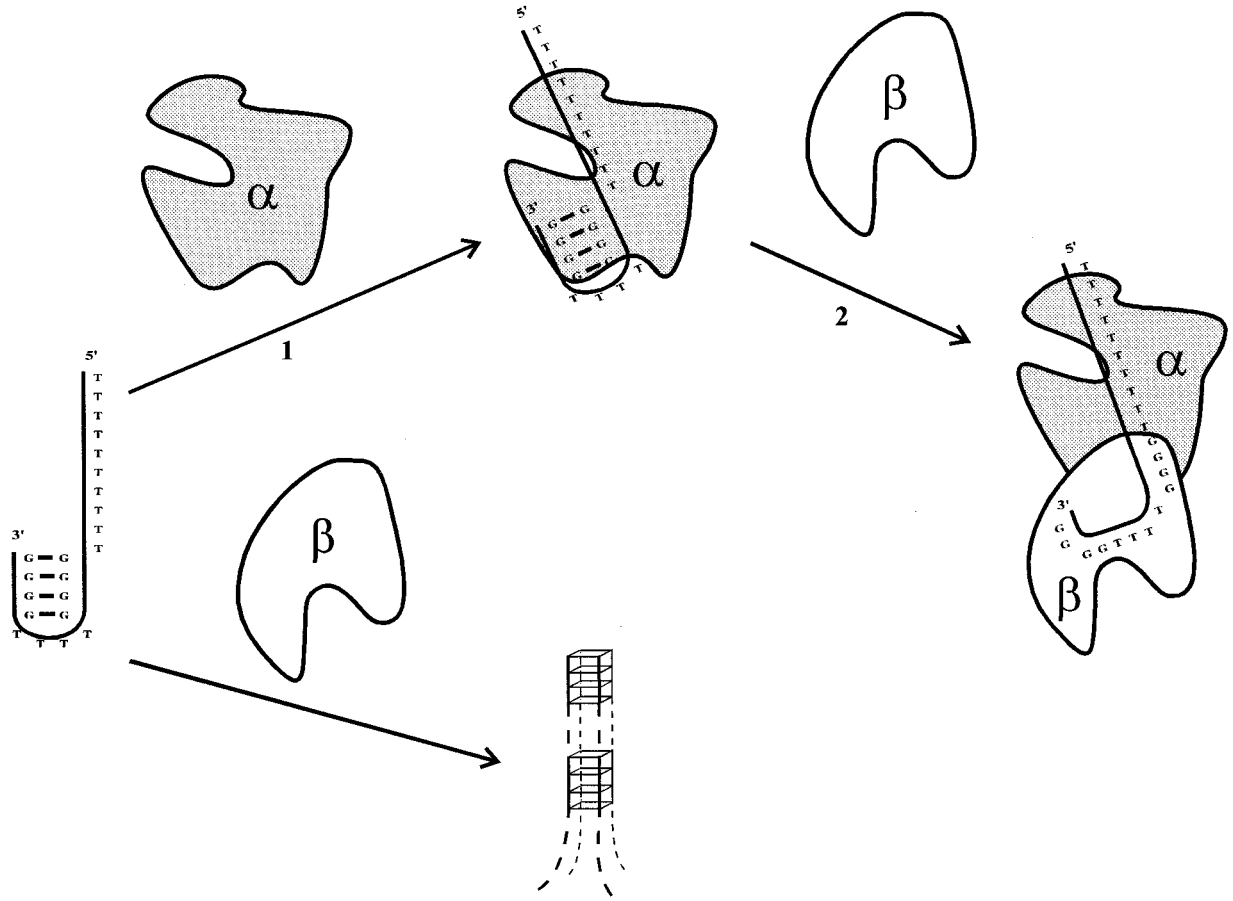

FIGURE 7: Schematic representation of the nature of telomeric DNA refolding induced by binding of the *Oxytricha* telomere binding protein. Top pathway: Sequential binding of both α and *β* subunits. Bottom pathway: Binding of only the *β* subunit (*14*). In the case of sequential binding, step 1 is supported by both spectroscopic (this work) and biochemical evidence (*17*), while step 2 is supported by biochemical studies (*17*). In the case of binding of only the *β* subunit, both spectroscopic (*14*) and biochemical studies (*15*, *16*) support quadruplex formation.

protein or the DNA component, respectively, is in stoichiometric excess. The Raman analysis of α:T6Oxy2 described above corresponds to the species with electrophoretic mobility of band c. The three lanes on the left in Figure 6 demonstrate that complexes formed by α with Oxy2, $d(TG)_8$, and $dT_6(TG)_8$ are electrophoretically different from the complex formed with T6Oxy2. The α:Oxy2 and α:$d(TG)_8$ complexes exhibit similar mobilities (band e), presumably indicative of similar charge distributions in the vicinity of the DNA binding site. Interestingly, this is consistent with the absence of hairpin formation (i.e., no G·G pairing) in both α:Oxy2 and α:$d(TG)_8$, as concluded from the Raman spectra. The lane corresponding to α:$T_6(TG)_8$ provides evidence of at least two major species (bands d and f) and possibly more. However, none of these exhibits evidence of sufficient DNA structure perturbation to alter either the Raman or the CD signature of the DNA component.

CONCLUSIONS

While the DNA binding mechanism of the *β* subunit of the *Oxytricha* telomere binding protein has been extensively characterized (*14*−*16*), the role of the α subunit has been much less studied. The present Raman and CD spectra provide new insights into the nature of telomeric DNA binding by the α subunit and suggest a physiologically relevant role for this subunit. The analysis given here makes use of the demonstrated ability of the *Oxytricha* telomeric repeat Oxy2, and of the related sequence, T6Oxy2, to form a hairpin secondary structure stabilized by G·G base pairs of the Hoogsteen type (*19*). We have exploited the distinctive Raman signature of this telomeric hairpin motif. The present study demonstrates that although the α subunit is capable of binding to telomeric sequences with and without a 5′ leader, highly specific DNA−protein interaction and substantial conservation of the telomeric hairpin fold are favored for the *Oxytricha* telomeric repeat that contains the 5′ leader.

Complexes formed by the α subunit with nontelomeric DNA isomers, such as $d(TG)_8$ and $dT_6(TG)_8$, and with a double-stranded DNA model, $d(C_4A_4C_4)$·$d(G_4T_4G_4)$ (unpublished results), exhibit either nonspecific interaction or no structural perturbation to the DNA strand and presumably occur by a nonspecific mechanism, possibly involving electrostatic interactions between basic side chains of the α subunit and phosphates of the DNA backbone. The binding of the α subunit to the *Oxytricha* telomeric repeat that lacks a 5′ leader (Oxy2) induces unfolding of the telomeric hairpin and may result in a complex similar to that occurring for nontelomeric sequences (Figure 6).

The results obtained here underscore the importance of the 5′-leading sequence in telomere-specific binding of the α subunit. Without the 5′ leader, the α subunit apparently fails to distinguish the telomeric repeat from nontelomeric isomers. We propose that the in vivo role of the α subunit is to prepare the telomeric repeat for formation of the α:*β*:

DNA ternary complex (*10*, *11*, *13*). It seems unlikely that the β subunit alone could fulfill a similar role, because it catalyzes the formation of parallel-stranded quadruplex structures (*14*−*16*). A schematic representation of possible roles of the α and β subunits in telomeric DNA recognition, organization, and function is shown in Figure 7.

In future work, the combined structural roles of the α and β subunits of the *Oxytricha* telomere binding protein in promoting ternary complex formation with *Oxytricha* telomeric DNA will be investigated.

ACKNOWLEDGMENT

We thank Professor Thomas R. Cech of the University of Colorado, Boulder, who generously provided plasmids and cells for expression of the *Oxytricha* telomere binding proteins. We also thank Dr. Christoph Krafft for helpful comments on the manuscript.

REFERENCES

1. Blackburn, E. H. (1994) *Cell 77*, 621−623.
2. Blackburn, E. H., and Greider, C. W., Eds. (1995) *The Telomeres*, CSHL Press, Cold Spring Harbor, New York.
3. Lundblad, V., and Szostak, J. W. (1989) *Cell 57*, 633−643.
4. Sandell, L. L., and Zakian, V. A. (1993) *Cell 75*, 729−739.
5. Raghuraman, M. K., Brewer, B. J., and Fangman, W. L. (1997) *Science 276*, 806−812.
6. Kirk, K. E., Harmon, B. P., Reichardt, I. K., Sedat, J. W., and Blackburn, E. H. (1997) *Science 275*, 1478−1481.
7. Marcand, S., Gilson, E., and Shore, D. (1997) *Science 275*, 986−990.
8. Griffith, J., Bianchi, A., and de Lange, T. (1998) *J. Mol. Biol. 278*, 79−88.
9. Sen, D., and Gilbert, W. (1990) *Nature 344*, 410−414.
10. Price, C. M., and Cech, T. R. (1987) *Gen. Dev.* 783−793.
11. Raghuraman, M. K., and Cech, T. R. (1989) *Cell 59*, 719−728.
12. Price, C., and Cech, T. (1989) *Biochemistry 28*, 769−774.
13. Gottschling, D. E., and Zakian, V. A. (1986) *Cell 47*, 195−205.
14. Laporte, L., and Thomas, G. J., Jr. (1998) *Biochemistry 37*, 1327−1335.
15. Fang, G., and Cech, T. R. (1993) *Biochemistry 32*, 11646−11657.
16. Fang, G., and Cech, T. R. (1993) *Cell 74*, 875−885.
17. Fang, G., Gray, J. T., and Cech, T. R. (1993) *Genes Dev. 7*, 870−882.
18. Laporte, L., Stultz, J., and Thomas, G. J., Jr. (1997) *Biochemistry 36*, 8053−8059.
19. Laporte, L., and Thomas, G. J., Jr. (1998) *J. Mol. Biol. 281*, 261−270.
20. Gray, J. T., Celander, D. W., Price, C. M., and Cech, T. R. (1991) *Cell 67*, 807−814.
21. Miura, T., and Thomas, G. J., Jr. (1995) *Biochemistry 34*, 9645−9654.
22. Thomas, G. J., Jr., and Barylski, J. R. (1970) *Appl. Spectrosc. 24*, 463−464.
23. Benevides, J. M., Kukolj, G., Autexier, C., Aubrey, K. L., DuBow, M. S., and Thomas, G. J., Jr. (1994) *Biochemistry 33*, 10701−10710.
24. Miura, T., and Thomas, G. J., Jr. (1994) *Biochemistry 33*, 7848−7856.
25. Thomas, G. J., Jr., and Tsuboi, M. (1993) *Advances in Biophysical Chemistry*, Volume 3, pp 1−70, JAI Press, Greenwich, CT.
26. Nishimura, Y., and Tsuboi, M. (1986) in *Spectroscopy of Biological Systems* (Clark, R. J. H., and Hester, R. E., Eds.) pp 177−231, John Wiley and Sons, London.
27. Fodor, S. P. A., Rava, R. P., Hays, T. R., and Spiro, T. G. (1985) *J. Am. Chem. Soc. 107*, 1520−1529.
28. Benevides, J. M., Weiss, M. A., and Thomas, G. J., Jr. (1994) *J. Biol. Chem. 269*, 10869−10878.
29. Thomas, G. J., Jr., and Benevides, J. M. (1985) *Biopolymers 24*, 1101−1105.
30. Balagurumoorthy, P., Brahmachari, S. K., Mohanty, D., Bansal, M., and Sasisekharan, V. (1992) *Nucleic Acids Res. 20*, 4061−4067.
31. Scaria, P. V., Shire, S. J., and Shafer, R. H. (1992) *Proc. Natl. Acad. Sci. U.S.A. 89*, 10336−10340.

BI9819024